Journal of the Serbian Chemical Society
JSCS-info@shd.org.rs • www.shd.org.rs/JSCS
J. Serb. Chem. Soc. 78 (7) 1055–1077 (2013)
JSCS–4481
UDC 661.183.6+54–145.2+544.723+544.4:632.95
Original scientific paper

Extractive efficacy for acephate of microwave synthesized zeolitic materials: equilibrium and kinetics

BHAVNA A. SHAH[1]*, AJAY V. SHAH[2] and PIYUSH Y. JADAV[1]

[1]*Department of Chemistry, Veer Narmad South Gujarat University, Surat-395007, Gujarat, India and* [2]*Science and Humanity Department, Polytechnic, Vidyabharti trust, Umrakh, Bardoli-394345, Gujarat, India*

(Received 30 May, revised 23 November 2012)

A*bstract*: The present investigation deals with the utilization of Bagasse fly ash (BFA), a sugar industry waste, and a zeolitic material (MZBFA) synthesized from BFA by a combined conventional and microwave reflux method as adsorbents for the extraction of acephate (ACP), an organophosphorus pesticide, from aqueous solution. The synthesized adsorbents were characterized using various techniques, such as Fourier-transform infrared (FTIR) spectroscopy, powder X-ray diffraction (PXRD) analysis and scanning electron microscopy (SEM). The effects of various experimental parameters were investigated using a batch adsorption technique for the extraction of ACP. The extent of removal increased with decreasing initial ACP concentration and particle size of the adsorbent. The adsorption was fast and equilibrium was established within 90 min. Pseudo-first-order, pseudo-second-order, Bangham and intra-particle diffusion models were used to fit the experimental data. The pseudo-second-order rate equation was able to provide a realistic description of the adsorption kinetics. Equilibrium isotherms were analyzed by the Freundlich, Langmuir, Dubinin–Radushkevich and Tempkin isotherm Equations. The Langmuir Equation was found to represent the equilibrium data the best. A thermodynamic study showed that the adsorption of ACP on MZBFA was higher than that on BFA. The results indicate that such Zeolitic materials could be employed as low cost alternatives to BFA in wastewater treatment for the removal of pesticides.

Keywords: ACP; adsorption; isotherm; kinetics; zeolite.

INTRODUCTION

In recent years, the application of organophosphorus pesticides to agricultural crops and other land areas has increased manifold. India is the largest consumer of pesticides of the South Asian countries with 44.5 % consumption of the

* Corresponding author. E-mail: bhavna606@gmail.com
doi: 10.2298/JSC120530146S

total pesticides for cotton crops alone.[1] Substantive application of pesticides may cause accumulation in the hydrological systems[2] and in food crops.[3,4] The leaching runoff from agricultural and forest lands, deposition from aerial applications, and discharge of industrial wastewater are responsible for water contamination.[5]

Pesticides are considered to be potential chemical mutagens and potential chronic health hazards.[6] Considerable evidence has been accumulated indicating contamination of natural water resources globally, including India.[7] The Poison information Center in National School of Occupational Health (NIOH), Ahmadabad, India, reported that organophosphorus compounds are responsible for maximum number of poisoning (73 %) among all agricultural pesticides.[7] Patients of acute organophosphorus poisoning have been reported to suffer from problems such as vomiting, nausea, miosis, excessive salivation, blurred vision, headache, giddiness and disturbance in consciousness.[8]

Acephate, *N*-(methoxy-methylsulfanylphosphoryl)acetamide, is one of the ten most important organophosphorus insecticides in terms of sales volume. It has been extensively used in cotton crop cultivation. Surface and ground water contamination have been observed due to the presence of acephate. For evaluation of environmental waters and water resources for preparation of drinking water, highly sensitive methods for the determination of organophosphorus pesticides in surface water, ground water and drinking water are required. In the European Union, a maximum allowable concentration of 0.1 μg L^{-1} for each individual (organophosphorus) pesticide in drinking water is in force. In the Netherlands, for aquatic ecosystems, the maximum allowable risk level for organophosphorus pesticides varies from 0.0007 to 23 μg L^{-1}.[9] Therefore, effective methods of pesticide removal from water are urgently needed. However, the wide ranges of pesticides, insecticides and herbicides in use make research extremely difficult for producing a single method for their removal. Several methods, either independent or in conjunction with others, have been used for the removal of pesticides, and these include chemical oxidation with ozone,[8] photodegradation,[10] UV irradiation,[11] biological degradation[11] and adsorption.[12–20] Adsorption on activated carbon is the most widely spread technology used for water treatment.[21] However, the commercially available carbon is not economically feasible on the large scale due to its high cost. For this reason, many industrial, agricultural, natural, and synthetic materials, such as bagasse fly ash (BFA), carbon cloth, porous polymeric adsorbents, wheat-residue black carbon, resin, lignin, wood charcoal, waste tire rubber granules, *etc*., have been converted into inexpensive activated carbons for this purpose.[21]

Despite many studies on the chemical modification of cellulose, only a few investigated the modification of bagasse fly ash. In view of all these facts, attempts were made to convert bagasse fly ash, a waste material of the sugar industry, into an inexpensive and effective adsorbent, such as zeolite. BFA is cur-

rently used as a filler in building materials. It was used previously for chemical oxygen demand (COD) reduction of sugar mill and paper mill effluents.[22] Various researchers utilized it for the adsorptive extraction of phenolic compounds,[23] metals[24,25] and dyes.[26] However, from the survey of the literature, no information for the adsorptive removal of ACP pesticide by BFA and a zeolitic material (MZBFA) synthesized from BFA could be found.

The main objective of this paper were: *i*) to study the feasibility of using BFA and MZBFA as adsorbents for the removal of ACP pesticide, *ii*) to determine the physicochemical characteristics and thermal stability of BFA and MZBFA, *iii*) to determine the various parameters affecting the sorption, such as pH, adsorbent dose, initial concentration, contact time and temperature, *iv*) to evaluate the usefulness of various kinetic models, *viz*. pseudo-first-order, pseudo-second-order, Bangham and intra-particle diffusion models and *v*) to determine the applicability of linear and non-linear forms for various isotherm models (*i.e*., the Freundlich,[27] Langmuir,[28] Dubinin–Radushkevich[29] and Tempkin models[30]).

EXPERIMENTAL

Preparation of adsorbents

In the present investigation, BFA was collected from a local sugar mill, Shree Khedut Sahkari Khand Udhyog Mandali Ltd., located at Bardoli, Gujarat, India. All of the reagents used in these investigations were supplied by Merck and Rankem as analytical grade reagents. Initially, the raw BFA obtained from the sugar mill was washed thoroughly with double distilled water to avoid the presence of foreign impurities and dried in sunlight for 8 and then 4 h in hot air oven at 353±5 K. The washed and dried material was sieved through a 200-µm mesh sieve to eliminate the larger particles. The dried BFA material, sieved through 200 µm mesh sieve was suspended into 3 M NaOH solution (8:1 liquid:solid ratio) for partial microwave irradiation at the earlier stages (15 min) followed by conventional heating (165 min) in a round bottom flask equipped with a reflux condenser and stirrer at a reaction temperature of 373±5 K. Microwave experiments were realized using a microwave oven (Q-ProM, Germany). After the hydrothermal reaction, the treated BFA was allowed to cool to room temperature. The resultant zeolite was washed with distilled water to remove excess sodium hydroxide, filtered and dried at 373±10 K in a hot air oven. The zeolization of bagasse fly ash by microwave heating was reported to be useful for shortening the reaction time (from hours or days down to minutes).

Instrumental techniques

A UV–Visible spectrophotometer (UV-1601, Shimadzu, Japan) was used to detect ACP. The pH measurements were made using a pH meter (PICO$^+$, Labindia pH meter, India). The Fourier-transform infrared (FTIR) spectra of the samples were recorded on a FTIR spectrophotometer (Thermo Nicolet IS10, Thermo Scientific Ltd., Switzerland). The specific surface area and pore volume of the adsorbents were determined using the Brunauer–Emmett–Teller (BET)[31] and Barret–Joyner–Halenda (BJH)[32] nitrogen adsorption and desorption methods at 77 K using a Micromeritics automatic surface area analyzer (Gemini 2360, Shimadzu, Japan). The chemical composition of each adsorbent was examined by the X-ray fluorescence method (X-ray XDL-B, Fischer scope, Japan). The moisture contents of the adsorbents were deter-

mined using a Karl-Fischer (1204R of VMHI, Metrohm Ltd., USA) instrument. The powder X-ray diffraction (PXRD) patterns of the adsorbents were obtained using a Panalyticals X-Pert Pro instrument employing nickel filtered Cu K_α (λ = 1.54060 Å) radiation. The density of the adsorbent was determined by pycnometery. The point of zero charge was calculated by the mass titration method.[33]

Adsorbate

High purity (99.1 %) ACP pesticide (obtained from United Phosphorous Ltd., India) was used as the adsorbate in the present study. The characteristics of ACP pesticide are listed in Table I. ACP is white crystalline powder with a strong mercaptan-like odor. Since ACP is hygroscopic, it was preserved in a dry atmosphere. An accurately weighed quantity of ACP was dissolved in distilled water to prepare stock solutions. The ACP solution was allowed to stand for some time until the absorbance of the solutions remained unchanged. Experimental solutions of desired pesticide concentration were obtained by successive dilutions.

TABLE I. The physical and chemical characteristics of ACP

Pesticide name	Abbreviation	IUPAC Name	λ_{max} nm	Empirical formula	Molecular mass, g mol^{-1}
Acephate	ACP	*N*-(methoxy-methylsulfanyl-phosphoryl)acetamide	214	$C_4H_{10}NO_3PS$	183.17

Analytical measurements

The UV–Vis spectrum of a standard solution ACP was recorded to determine its maximum absorbance (λ_{max}), which was found to be at 214 nm. A calibration curve for ACP was plotted between the absorbance 214 nm and the concentration of standard ACP solutions. The ACP concentrations were calculated from the calibration curve.

Batch experimental studies

To study the effect of important parameters on the adsorptive removal of ACP, batch experiments were conducted. For each experimental run, 50 mL of ACP of known concentration, pH and the known amount of the BFA and MZBFA were taken in a 100 mL brown colored glass bottle. The mixture was agitated in an incubator shaker at a constant speed of 150 revolutions per min. Samples were withdrawn at appropriate time intervals and the withdrawn samples were filtered and spectrophotometrically analyzed for the residual ACP concentration. Experiments were performed at initial pH values ranging from 2–10; controlled by the addition of 1 M HCl or 1 M NaOH solutions. For optimum amount of adsorbents per unit mass adsorbate, a 50 mL ACP solution was contacted with different amounts of adsorbents (1–6 g L^{-1}) until equilibrium was attained. Kinetics of adsorption was determined by analyzing adsorptive uptake of the ACP from the aqueous solution at different time intervals. For adsorption isotherms, ACP solutions of different concentrations (50–200 mg L^{-1}) were agitated with known amount of adsorbents until equilibrium was achieved. The residual ACP concentration was then determined. Blank runs, with only the adsorbents in 50 mL of distilled water were conducted simultaneously under similar conditions to account for any adsorption by either the container or the filter material. Each experiment was repeated three times and the mean values were taken.

RESULTS AND DISCUSSION

Characterization of adsorbents

Characteristics of adsorbents were determined by proximate analysis and physicochemical properties. Results are presented in Table II. The formation mechanism of zeolitic material from BFA was previously proposed as follows: dissolution of SiO_2 and Al_2O_3, particularly from the glass phase, into the alkaline solution, decomposition of aluminosilicate gel as zeolite precursor, and crystallization of zeolite. In present study, mechanism of zeolization is mainly separated into three terms. The first step is dissolution of SiO_2 and Al_2O_3 into the alkaline solution at 0–15 min. After 15 min, an intermediate aluminosilicate gel forms by the deposition of dissolved Si and Al species, which is the prematerial of zeolite crystals covering the external surface of BFA particles. The intermediate gel begins to change into zeolite *via* a dissolution–reprecipitation process at 40 min and the capture of sodium ions to neutralize the negative charge on the aluminate in the zeolite structure when zeolite crystal growth occurred. Zeolization was enhanced by partial microwave irradiation in the early stages of reaction because microwave can rapidly heat up an aqueous solution. Another reason may be assigned to active water generated by the break up of hydrogen bonds under microwave irradiation. The active water molecules, isolated H_2O molecules, should freely attack Si–O and Al–O bonds so to enhance the dissolution of the glass phase on the fly ash particles. The particle size of synthesized MZBFA and native BFA were determined by a Mastersizer 2000 particle size analyzer. The particle size distributions specify that majority of particles lies below 58.55 μm (95 %) in case of MZBFA, while in BFA majority of particles lies below 150.62 μm (95 %). The surface area of BFA and MZBFA were determined by the BET nitrogen adsorption method. The specific surface area obtained by the instrument for BFA and MZBFA were 99.14 and 328.30 $m^2\ g^{-1}$ respectively. This indicates that the surface area of zeolitic adsorbent had been increased significantly during treatment. The mass titration results for BFA and MZBFA are shown in Fig. 1. The pH_{pzc} values obtained by mass titration method were 8.18 and 9.09 pH for BFA and MZBFA, respectively.

TABLE II. Physicochemical properties of BFA and MZBFA

Characteristics	Obtained values	
	BFA	MZBFA
Proximate analysis, mass %		
Loss on drying	11.95±0.2	13.74±0.2
Moisture content	10.36±0.3	12.25±0.3
Ash content	72.85±0.2	67.74±0.2
Physical properties		
Specific density	1.888±0.02	2.036±0.02

TABLE II. Continued

Characteristics	Obtained values	
	BFA	MZBFA
Physical properties		
Bulk density, g mL^{-1}	1.725±0.02	1.983±0.02
Dry density, g mL^{-1}	1.081±0.02	1.225±0.02
Void ratio	0.747	0.662
Porosity, fraction	0.428	0.398
pH_{pzc}	8.18±0.05	9.09±0.05
BET Surface area	99.14	328.30
Composition, mass %		
SiO_2	46.35	43.54
Al_2O_3	19.99	18.90
Fe_2O_3	5.89	2.99
CaO	4.97	3.17
MgO	4.83	4.12
Na_2O	4.17	7.24
K_2O	3.74	2.35

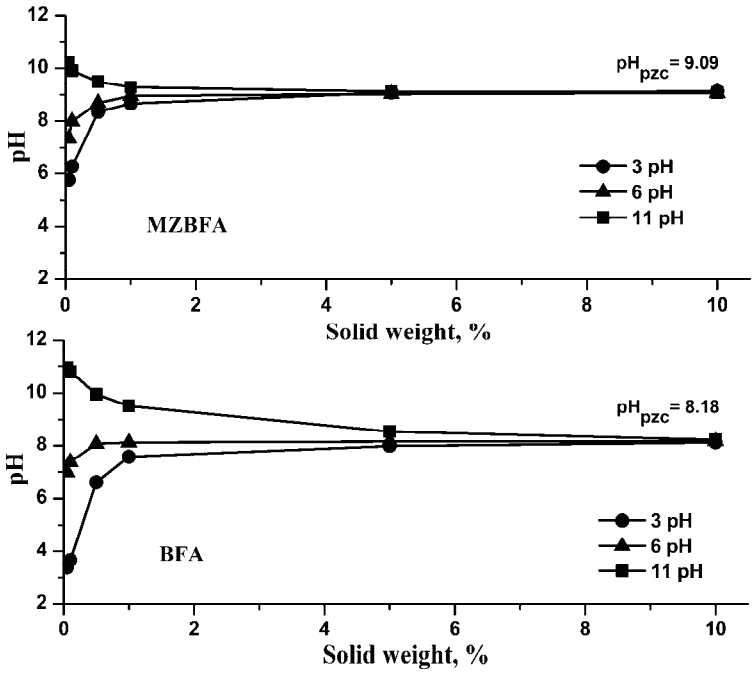

Fig. 1. Mass titration curves of BFA and MZBFA.

FT-IR Analysis

FT-IR spectra of the adsorbents, shown in Fig. 2, exhibit a broad band at about 3400 cm^{-1} indicating the presence of both free and hydrogen bonded OH

groups on the adsorbent surface; the stretching is due to both silanol groups (Si–OH) and adsorbed water on the surface of adsorbents. The 1033.97, 676.67 and 475.33 cm^{-1} bands are due to the asymmetric stretching vibration of the internal tetrahedra, the symmetric stretching vibration and the bending vibration modes of T–O bonds in the TO_4 tetrahedra (where T = Si or Al), respectively. The band at 1097.31 cm^{-1} of BFA was shifted to 1033.97 cm^{-1} in MZBFA, confirming the tetrahedral coordination of aluminum in the zeolite skeleton. In MZBFA, the shift of the symmetric stretching band at 797.53 to 792.61 cm^{-1} of the internal tetrahedral (TO_4) of the amorphous aluminosilicates formed by the reaction of dissolved Si^{4+} and Al^{3+} confirmed the formation of zeolite phases.[34,35] The amount of improved tetrahedral sites of the aluminosilicate skeleton of the zeolite can be seen by the decreased frequency of the asymmetric stretching vibration of the tetrahedral. The band at about 1646.21 and 1456.34 cm^{-1} are ascribed to deformation of the –OH vibration of absorbed water and the bending vibration of interstitial water.[34]

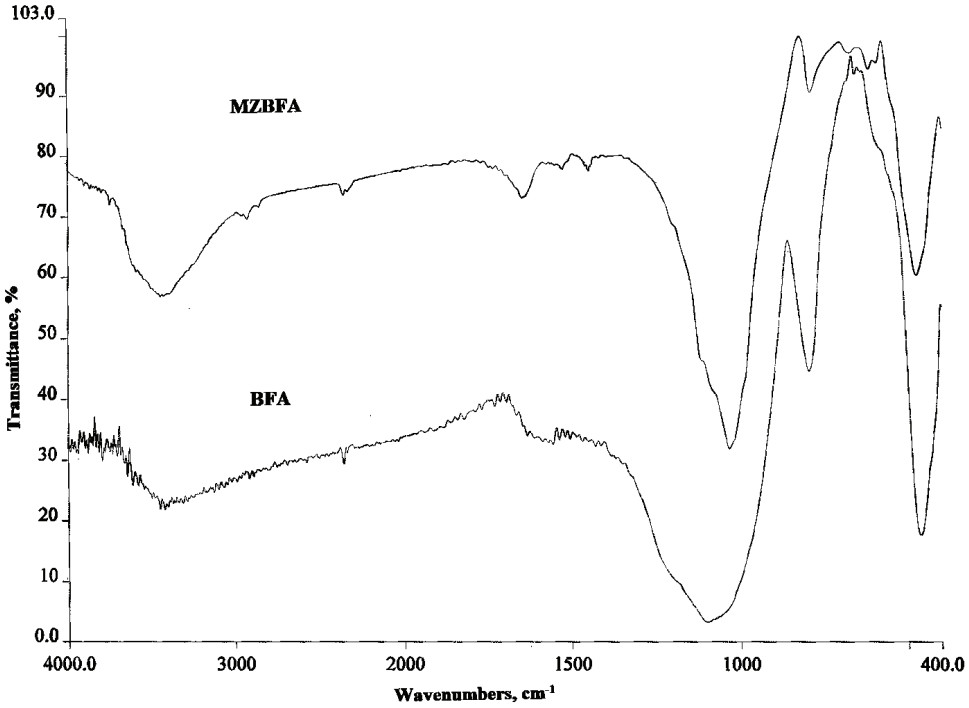

Fig. 2. FTIR Spectra of BFA and MZBFA.

PXRD Analysis

The identification of corresponding crystalline and mineralogical characteristics of adsorbents were made from powder X-ray diffraction patterns by

comparing the diffraction data against a database provided by "Joint Committee on Powder Diffraction Standards".[36] The low hump at lower diffraction angle in the BFA diffraction patterns shown in Fig. 3 indicates the presence of a glass phase.[37] BFA exhibited the presence of α-quartz as the major part and other amorphous materials.[36] The PXRD pattern of MZBFA showed that the hump at lower diffraction angle was suppressed. The newly observed intense peaks at 2θ 26.54 and 43.09° can be ascribed to the formation of zeolites in MZBFA. The X-ray diffraction patterns of MZBFA confirmed the presence of zeolite P (Phillipsite, JCPDS 39-0219) and zeolite X (JCPDS 28-1036) as the major minerals as indicated from their high intensities as seen in Fig. 3. Analcime (JCPDS 76--0901), zeolite A (JCPDS 14-90), chabazite (JCPDS 12-0194) and ZSM 12 (JCPDS 15-274) were present as minor minerals.

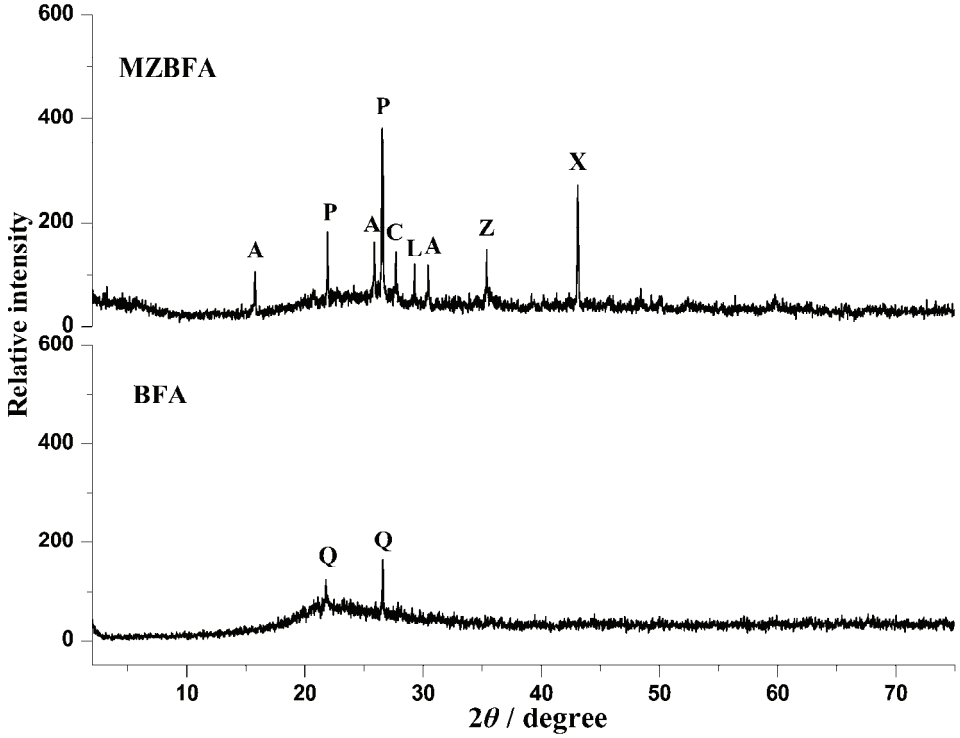

Fig. 3. PXRD Patterns of BFA and MZBFA. (P = phillipsite, X = zeolite X, A = analcime, L = zeolite A, Z = ZSM-12, C = chabazite and Q = α-quartz).

Morphology of the adsorbents

The SEM photomicrographs of both the adsorbents at 5.00 KX magnifications are presented in Fig. 4. The SEM image of BFA before hydrothermal reaction mostly contains non-crystalline glass, with a loose structure and posses smooth

surface particle with no pits because the surface is covered by an aluminosilicate glass phase. The particles of MZBFA appeared to be more fluffy and porous. The SEM photomicrograph of MZBFA shows clear crystalline forms with compact structures and honeycomb aperture and holes. The MZBFA image shows the development of extended folded strands with deeper pits; with interior voids. The SEM photomicrograph of the pesticide loaded adsorbents shown in Fig. 4 reveals that the layered strands become diminished, showing that the adsorption of the pesticide created a more compact nature and spherical beads fill up the surface showing very intense pesticide adsorption on the surface throughout. In the case of MZBFA, agglomeration of particles forming clusters could be expected due to its softer porous texture.

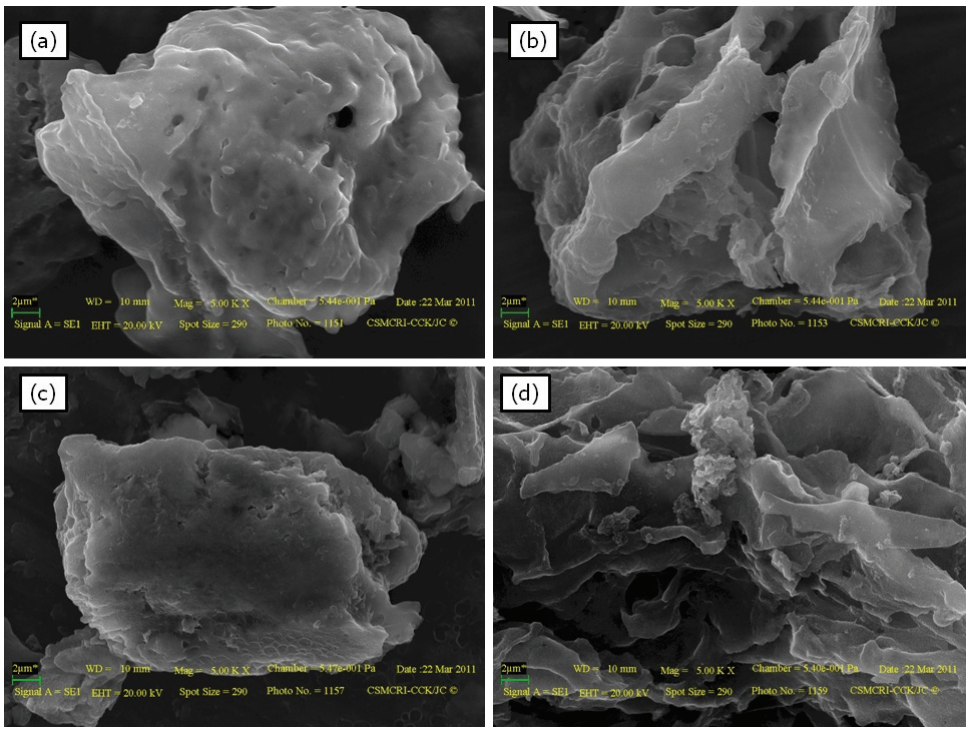

Fig. 4. SEM Micrographs of a) BFA, b) MZBFA, c) ACP-loaded BFA and d) ACP-loaded MZBFA at 5000× magnification.

Effect of pH

The adsorption of ACP by BFA and MZBFA was studied over a pH range of 2–10 at 298 K for 6 h. The initial ACP concentration was 125 mg L^{-1} and the adsorbent doses were kept at 0.15 g 50 mL^{-1}. The effects of pH on the adsorptive removal of ACP by the adsorbents are shown in Fig. 5. The pK_a of ACP is 8.35

and ACP exists in molecular form below this pH. The pH_{pzc} of the MZBFA increased to 9.09 from 8.18 in case of BFA, due to the alkaline hydrothermal treatment, which enables the utilization of MZBFA over a wide pH range, suitable for the adsorption of pesticides. At acidic pH values, the adsorption affinities of the adsorbents toward ACP are high due to dispersive interactions that are promoted in solutions of pH below the pH_{pzc} of the adsorbents. The percentage removal of ACP was maximum at acidic pH (pH 2), decreased with further increase in pH (up to pH 6) for both adsorbents and after pH 6 a trivial increase was observed up to 10 pH. At pH < pH_{pzc}, the negatively charged silica sites of the adsorbent are neutralized by H^+, thereby reducing hindrance to the diffusion of ACP ions. For the pH below 4, a significantly high electrostatic attraction exists between the positively charged surface of the adsorbent and appreciably ionized ACP. At pH 6, the partially charged ACP exhibits minimum adsorption on both adsorbents. As the pH of the system increases, the negative charge of adsorbent increases which results in high electrostatic repulsion between the solute molecules and between the solute and adsorbent surface. The percentage removal of ACP by BFA and MZBFA were 23±1 % and 33±1 %, respectively, at pH 2 after 6 h. The higher adsorption capacity of MZBFA compared to BFA in acidic solutions was due to the microporous structure of MZBFA, where ACP can be intensively adsorbed by the micropore-filling mechanism.[38]

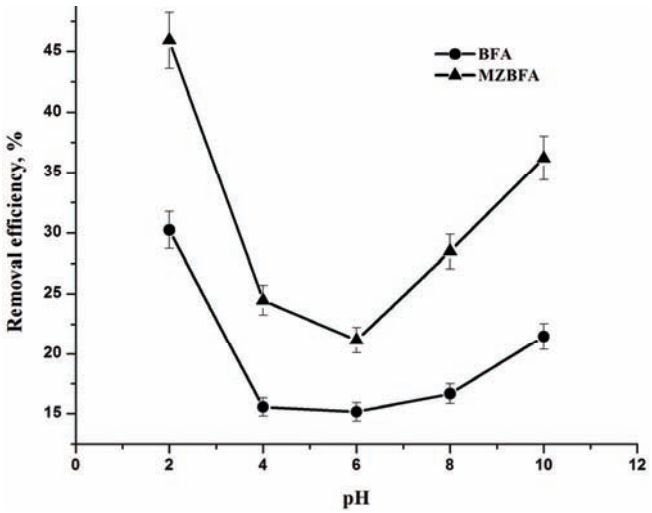

Fig. 5. Effect of pH (conc. = 125 mg L^{-1}, dose = 3 g L^{-1}, pH = 2–10, temperature = 298 K, time = 6 h) on the adsorption of ACP by BFA and MZBFA.

Effect of adsorbent dosage and acephate concentration

Initially, the rate of removal of ACP was found to be rapid, after which it slowed down as the dose concentration was increased, as shown in Fig. 6. The

removal efficiency became almost constant and no significant change was observed in the removal of ACP above 0.2 g 50 mL^{-1} in the solution. Thus, the results obtained from this section of the experiments indicated 37±1 and 56±1 % removal of ACP was observed by BFA and MZBFA, respectively, at a dose of 4 g L^{-1}. At higher doses, the remaining ACP concentration in the solution was expected to be very low, so it experiences high resistance to mass transfer.

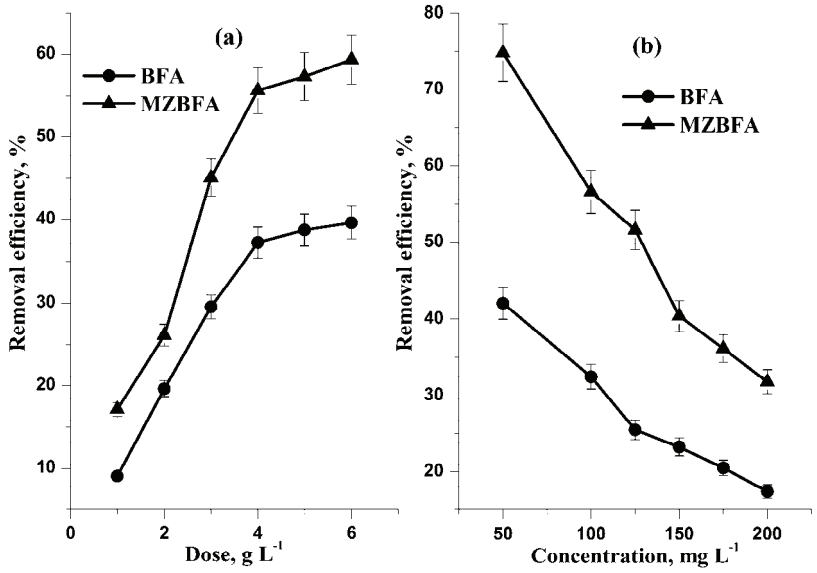

Fig. 6. a) Effect of adsorbent dosage (c = 125 mg L^{-1}, dose = 1–6 g L^{-1}, pH 2, temperature, 298 K, time, 5 h) and b) acephate concentration (c = 50–200 mg L^{-1}, dose = 3 g L^{-1}, pH 2, temperature, 298 K, time, 5 h) on the adsorption of ACP by BFA and MZBFA.

A given mass of adsorbent can adsorb only a fixed amount of adsorbate. Thus, the initial concentration of adsorbate solution is very important. The effect of the initial pesticide concentration on the removal by both the adsorbents is shown in Fig. 6. However, the amount of pesticide adsorbed per unit adsorbent mass increased with decreasing initial pesticide concentration due to the decrease in resistance to the uptake of solute from the pesticide solution. The curves indicate that the uptake efficiency of ACP by MZBFA was higher compared to that of BFA.

Effect of contact time

The effect of contact time on the adsorption of ACP by the adsorbents was studied for a period of 24 h for an initial pesticide concentration of 125 ppm at 298 K and pH 2. ACP solutions were kept in contact with the adsorbents for 24 h although no significant variation in the residual ACP concentration was detected

after a contact time of 5 h. Thus, after 5 h contact time, a steady-state approximation was assumed. The effect of the contact time on the adsorption of ACP is presented in Fig. 7. The contact time curve shows that the pesticide removal was rapid in the first 90 min. An early and rapid uptake of pollutant and the establishment of equilibrium in a short period signify the efficacy of an adsorbent for its use in wastewater treatment. The curves indicate possible monolayer coverage of the surface of adsorbents by the pesticide. In between these two uptake stages, the rate of adsorption was found to be nearly constant. This is understandable from the fact that a large number of vacant surface sites were available for adsorption during the initial stages, and after a lapse of time, the remaining vacant surface sites were difficult to occupy due to repulsive forces between the solute molecules on the solid and in the bulk phases. Saturation of BFA occurred at 25±1 % adsorption, while for MZBFA, it occurred at 53±1 % adsorption. The resulting data shows that MZBFA has a greater potential to adsorb ACP than BFA. This may be due to the higher surface area and larger pore volume of MZBFA as compared to BFA.

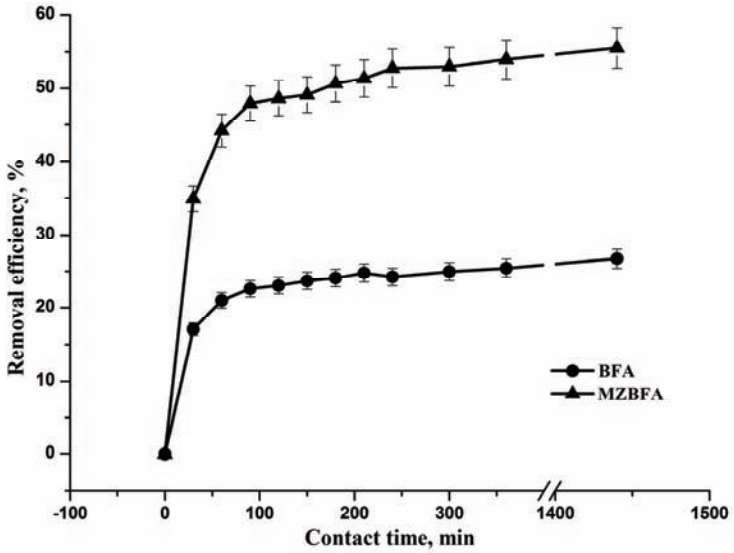

Fig. 7. Effect of contact time (c = 125 mg L^{-1}, dose = 3 g L^{-1}, pH 2, temperature, 298 K, time, 24 h) on the adsorption of ACP by BFA and MZBFA.

Effect of temperature and thermodynamic parameters

The adsorption of ACP on both the adsorbents was investigated at five different temperatures (293, 303, 313, 323 and 333 K). The uptake of ACP increased with increasing temperature, indicating the process is endothermic in nature.

Thermodynamic parameters were evaluated from Van't Hoff plots (not shown) for the adsorption of ACP onto BFA and MZBFA. The results are summarized in Table III. The change in enthalpy, ΔH^0, and change in entropy, ΔS^0, were evaluated from the slope and intercept, respectively, of the equation:

$$R \ln K_d = \frac{-\Delta G^0}{T} = \Delta S^0 - \frac{\Delta H^0}{T} \quad (1)$$

where, K_d is the distribution coefficient; ΔH^0 is the enthalpy change, kJ mol^{-1}; ΔS^0 is the entropy change, J K^{-1} mol^{-1}; R is the gas constant, 8.314 J mol^{-1} K^{-1} and T is the temperature, K.

The spontaneity of the adsorption process was ensured by the decrease in the Gibbs free energy, ΔG^0, of the systems. The negative values of ΔG^0 indicate that the adsorption process becomes more spontaneous with increasing temperature, which favors the adsorption process. The positive values of ΔH^0 were in the range of 6.04–7.40 kJ mol^{-1}, *i.e.*, lower than 20 kJ mol^{-1}, confirming the endothermic nature of the overall adsorption process and also the adsorption to be physical rather than chemical linking through weak attraction forces.[39,40] The positive value of ΔS^0 corresponds to an increase in the degree of freedom of the adsorbed species, signifying weak interaction between ACP and the adsorbents.[40] However, if the adsorption process is influenced by cylindrical and convective diffusion, the adsorption capacity will increase with temperature.[41] Furthermore, it may be due to an increase in the equilibrium constant with increasing temperature.

TABLE III. Thermodynamic parameters for the adsorption of ACP on BFA and MZBFA

Pesticide	$-\Delta G^0$ / kJ mol^{-1}					ΔH^0	ΔS^0
	T / K					kJ mol^{-1}	J mol^{-1} K^{-1}
	293	303	313	323	333		
BFA	7.199	7.811	8.309	8.660	9.028	6.035	45.48
MZBFA	9.217	9.698	10.24	10.94	11.43	7.403	56.58

Adsorption equilibrium studies

To optimize the design of an adsorption system for the adsorption of ACP, it is important to establish the most appropriate correlation for the equilibrium curves. Various linear and non-linear isotherm equations have been used to describe the equilibrium nature of adsorption. Some of these equations are the Freundlich,[27] Langmuir,[28] Dubinin–Radushkevich[29] and Tempkin[30] Equations. The models for characterization of the equilibrium distribution relate the quantity of solute adsorbed at equilibrium per unit weight of adsorbate, (q_e, mg g^{-1}) and the concentration of the solute remaining in the solution at equilibrium (c_e, mg L^{-1}).

The Freundlich isotherm[27] is derived by assuming a heterogeneous surface with a non-uniform distribution of heat of adsorption over the surface. The Freundlich isotherm was tested using the following linear equation:[27]

$$\log q_e = \log K_f + 1/n \log c_e \quad (2)$$

where q_e is the amount adsorbed (mg g^{-1}), c_e is the equilibrium concentration of the adsorbate (mg L^{-1}), and K_f and n are the Freundlich constants related to adsorption capacity and adsorption intensity, respectively. The values of R^2 for this model, Table IV, show that the Freundlich Equation presents the poorest fit of the experimental data compared to the other isotherm equations. Values of the heterogeneity factor $n > 1$ would indicate conformity of the data to the formation of a multilayer at the adsorbent surface. The reported data of adsorption of ACP on soil shows $K_f = 0.21$ and $n = 0.55$ which indicates multilayer formation is not possible in soil.[42] The value of n for the adsorption of ACP was higher for MZBFA (4.48) than for BFA (3.38).

The Langmuir Equation[28] can be used in following linearized form:

$$1/q_m = 1/Q_0 + 1/Q_0 B c_e \quad (3)$$

where q_m is the amount adsorbed (mg g^{-1}), c_e is the equilibrium concentration of the adsorbate (mg L^{-1}), and Q_0 and B are the Langmuir constants related to maximum adsorption capacity and energy of adsorption, respectively.

TABLE IV. Isotherm parameters for the adsorption of ACP on BFA and MZBFA

Isotherms	Adsorbent	Parameter values			
		q_m / mg g^{-1}	B / dm^3 mg^{-1}	R_L	R^2
Langmuir	BFA	13.699	0.044	0.155	0.990
	MZBFA	22.727	0.122	0.062	0.996
Freundlich		K_f / dm^3 g^{-1}	n	–	R^2
	BFA	10.328	3.38	–	0.875
	MZBFA	106.170	4.48	–	0.855
D–R		X_m / mg g^{-1}	B / mol^2 J^{-2}	E / kJ mol^{-1}	R^2
	BFA	8.166	5.1×10^{-4}	0.313	0.933
	MZBFA	15.975	1.5×10^{-4}	0.572	0.988
Tempkin		K_T / dm^3 mg^{-1}	B_1	–	R^2
	BFA	0.541	2.738	–	0.891
	MZBFA	3.107	3.677	–	0.860

Table IV indicates that the Langmuir model gave high quality fitting with correlation coefficient values R^2 0.990 to 0.996, *i.e.*, closer to unity than the other isotherms for the adsorption of ACP on BFA and MZBFA, indicating that the adsorption data better fits to the Langmuir isotherm model. Using the Langmuir model, the monolayer capacity of the adsorbents follows the order: MZBFA (22.73 mg g^{-1}) > BFA (13.70 mg g^{-1}). An essential characteristic of the Lang-

muir isotherm is that can be expressed in terms of a dimensionless separation factor, R_L, that was less than unity for both absorbents, which evidences that the adsorptions were favorable under the applied conditions. The relatively smaller value of R_L for adsorption by MZBFA than by BFA indicates that the adsorption was more feasible in the former case.

The Dubinin–Radushkevich (D–R) isotherm model[29] assumes that the mechanism of adsorption in micropores is pore-filling in nature, rather than layer-by-layer formation of a film on the walls of the pores. In order to appreciate the nature – physical or chemical – of the adsorption process, the isotherms data were analyzed by the (D–R) model, expressed by the following equation:[29]

$$\ln q_e = \ln X_m - \beta\varepsilon^2 \quad (4)$$

where q_e is the amount adsorbed (mg g^{-1}), X_m is the D–R monolayer capacity, β is the activity coefficient related to mean sorption energy, and ε is the Polanyi Potential, which is given by:

$$\varepsilon = RT \ln (1 / c_e) \quad (5)$$

where R is the gas constant (kJ mol^{-1} K^{-1}), T is temperature (K), and c_e is the equilibrium concentration of the adsorbate (mg L^{-1}). When ln q_e is plotted against ε^2, a straight line is obtained. The slope of the plot gives the value of β and the intercept yields the value of the sorption capacity, X_m (8.17–15.97 mg g^{-1}), as shown in Table IV. The value of β is related to sorption energy, E, *via* the following relationship:

$$E = \frac{1}{\sqrt{-2\beta}} \quad (6)$$

The magnitude of the adsorption energy, E, is related to the reaction mechanism. If E is in the range of 8–16 kJ mol^{-1}, the adsorption is governed by ion exchange. In the case of E < 8 kJ mol^{-1}, physical forces may affect the sorption mechanism. The calculated values E for the systems examined in the present study were found to be < 8 kJ mol^{-1} (Table IV), which indicates that the adsorption of ACP in the studied adsorbate–adsorbent systems was physical in nature.

The Tempkin isotherm[30] contains a factor that explicitly takes into account adsorbate species–adsorbent interactions. This isotherm assumes that: *i*) the heat of adsorption of all the molecules in the layer decreases linearly with coverage due to adsorbate species–adsorbent interactions and *ii*) the sorption is characterized by a uniform distribution of binding energies, up to some maximum binding energy. Thus:

$$q_e = B_1 \ln K_T + B_1 \ln c_e \quad (7)$$

where B_1 = RT b^{-1} and K_T are constants. K_T is the equilibrium binding constant (L mol^{-1}) corresponding to maximum binding energy and constant B_1 is related

to the heat of sorption. A plot of q_e *vs*. ln c_e enables the determination of the isotherm constants K_T and B_1.

The values of K_T and B_1 obtained from the Tempkin plots of q_e *vs*. ln c_e are presented in Table IV. The R^2 value obtained for MZBFA is very close to its value for the Freundlich isotherm. This indicates that the heat of sorption of all the molecules in the layer decreases linearly with coverage due to adsorbent–adsorbate interactions. Thus, the adsorption of ACP on MZBFA could be characterized by a uniform distribution of the binding energies, up to some maximum binding energy.

The non-linear fitting of all four isotherms for the BFA and MZBFA adsorbents are presented in Fig. 8. The non-linear curves of the isotherms also indicate

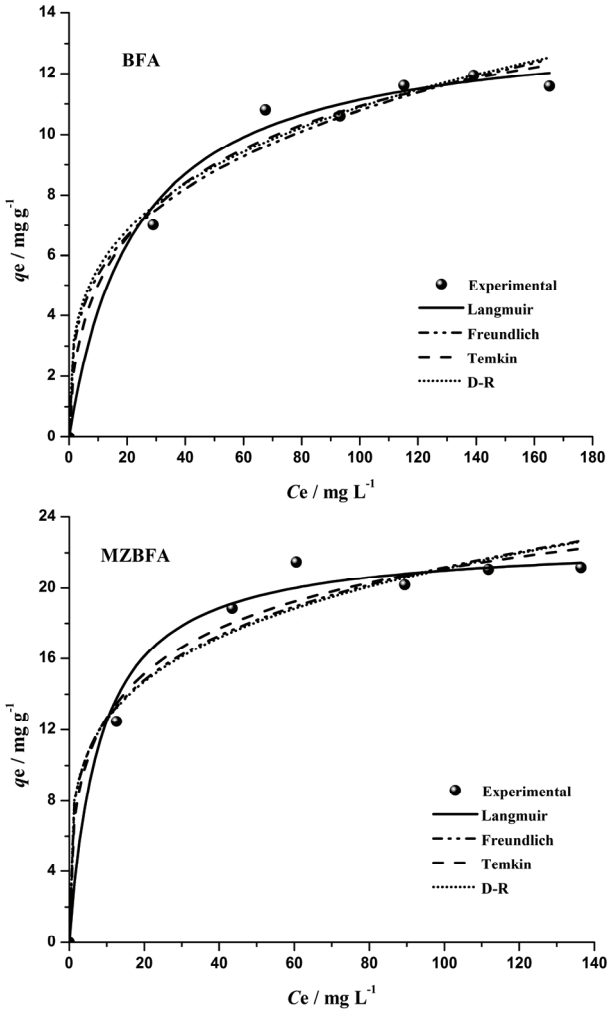

Fig. 8. Isotherms obtained using the non-linear method for the sorption of ACP onto BFA and MZBFA.

that of all four isotherms, the Langmuir Isotherm best fitted the experimental data. No matter what type of error distribution compromised the data; non-linear regression always produced accurate and efficient estimates of the parameters.[43] The adsorption equilibrium data of ACP onto both the adsorbents followed the order Langmuir > D–R > Tempkin ≥ Freundlich.

Adsorption kinetics

In order to investigate the adsorption process of ACP onto the adsorbents, four kinetic models were used, *i.e.*, the Lagergren pseudo-first-order,[44] the pseudo-second-order,[45] the Bangham[46] and the intra-particle diffusion[47] models. The pseudo-first-order kinetics model assumes that the rate of change of adsorbate uptake with time is directly proportional to the difference in the saturation concentration and the amount of solute uptake with time. The Lagergren Equation is given by:[44]

$$\log\left(q_e - q_t\right) = \log q_e - \left(\frac{k_f}{2.303}\right)t \tag{8}$$

where, q_t and q_e (mg g^{-1}) are the amounts of ACP adsorbed at time t (min) and at equilibrium, respectively, and k_f is the pseudo-first-order rate constant (min^{-1}) of the reaction.

A plot of log ($q_e - q_t$) *vs.* t, was drawn to express the Lagergren first order kinetics model (Fig. 9). The kinetic parameters calculated from the slope and intercept are given in Table V. These values indicate that the adsorption rate was very fast at the beginning of the adsorption for both adsorbents. The values of the equilibrium adsorption capacity, q_e, were well below the monolayer capacities found by the Langmuir equilibrium isotherm model. The q_e values suggested that the adsorption process was not a true first order reaction.

The rate of pseudo-second-order reaction is expressed by the following equation:[45]

$$\frac{t}{q_t} = \frac{1}{(k_s q_e^2)} + \frac{1}{q_e}t \tag{9}$$

where k_s is the rate constant of pseudo-second-order adsorption (g mg^{-1} min^{-1}) and $k_s q_e^2 = h$ can be regarded as the initial sorption rate (mg g^{-1} min^{-1}). The initial sorption rate, h; the equilibrium adsorption capacity, q_e; and the pseudo-second-order constant, k_s, can be determined experimentally from the slope and intercept of a plot of t/q_t *vs.* t (Fig. 9). The kinetic parameters along with the correlation coefficients for the pseudo-second-order kinetic model are listed in Table V. The obtained results revealed that the initial adsorption rate, h was fast and that the adsorption mechanism was somewhat complex and not a single step process. The correlation coefficients are closer to unity for the pseudo-second-order

kinetics than those for the pseudo-first-order kinetic model. Therefore, the adsorption of ACP by BFA and MZBFA could be approximated more appropriately by the pseudo-second-order kinetic model than by the pseudo-first-order kinetic model.

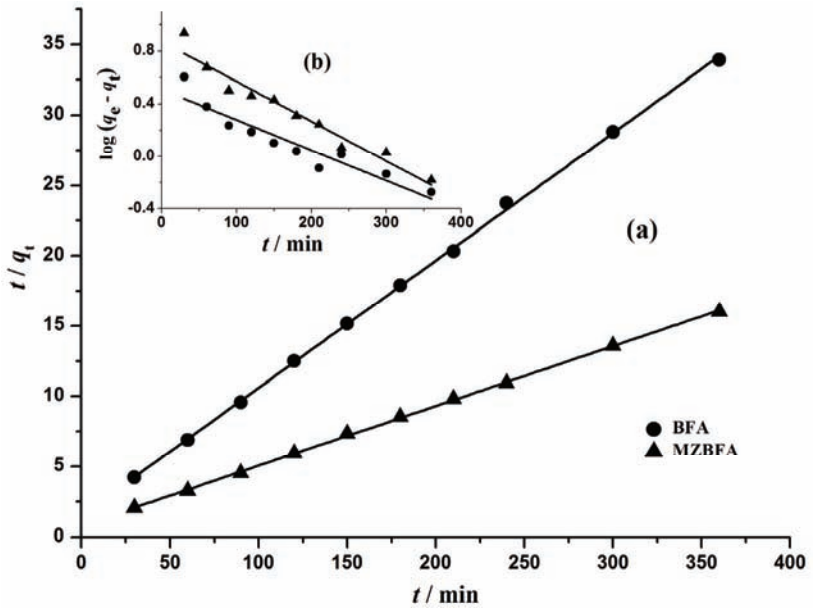

Fig. 9. a) Pseudo-second-order kinetic model (t/q_t *vs.* time) and b) pseudo-first-order kinetic model (log ($q_e - q_t$) *vs.* time) on the adsorption of ACP by BFA and MZBFA (c = 125 mg L^{-1}, dose = 3 g L^{-1}, temperature, 298 K).

TABLE V. Kinetic parameters for the removal of ACP by BFA and MZBFA

Pseudo-first order						
Adsorbent	q_e / mg g^{-1}	$k_f \times 10^3$ / min^{-1}	R^2			
BFA	3.236	4.606	0.897			
MZBFA	7.447	6.909	0.950			
Pseudo-second order						
Adsorbent	q_e / mg g^{-1}	$k_s \times 10^3$ / g mg^{-1} min^{-1}	h / mg g^{-1} min^{-1}	R^2		
BFA	11.111	5.364	0.060	0.999		
MZBFA	23.810	2.227	0.053	0.999		
Bangham						
Adsorbent	α	k_0 / g	R^2			
BFA	0.165	0.577	0.903			
MZBFA	0.216	1.141	0.909			
Intraparticle diffusion						
Adsorbent	$k_{id,1}$ / mg g^{-1} min$^{-1/2}$	I_1 / mg g^{-1}	R^2	$k_{id,2}$ / mg g^{-1} min$^{-1/2}$	I_2 / mg g^{-1}	R^2
BFA	0.582	4.017	0.974	0.114	8.465	0.888
MZBFA	1.367	7.290	0.972	0.290	17.120	0.947

The kinetic data were further employed to gain insight into the slow step occurring in the present adsorption system and to check whether the adsorption process was diffusion controlled by using the Bangham Equation:[46,48]

$$\log \log\left(\frac{c_0'}{c_0' - q'm'}\right) = \log\left(\frac{K_0 m'}{2.303\ V}\right) + \alpha \log t \qquad (10)$$

where c_0' is the initial concentration of adsorbate in solution (mmol L^{-1}), V is the volume of the solution (mL), m' is the weight of the adsorbent (g L^{-1}), q' is the amount of adsorbate retained at time t (mmol g^{-1}), and α and k_0 are constants. The values of constants α (<1) and k_0 are given in Table V. The double logarithmic plot (Fig. 10) according to above equation did not yield perfect linear curves (R^2 = 0.903 and 0.909 for removal of ACP by BFA and MZBFA, respectively, because the diffusion of adsorbate into the pores of the sorbents was not the only rate controlling step.

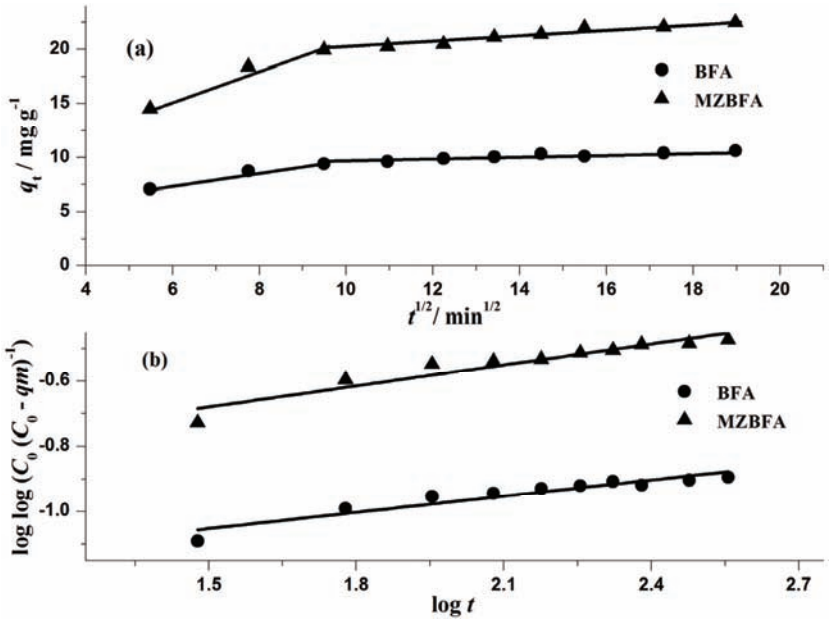

Fig. 10. a) Intra-particle diffusion plots and b) Bangham plots on the adsorption of ACP by BFA and MZBFA (c = 125 mg L^{-1}, dose = 3 g L^{-1}, temperature, 298 K).

The possibility of intra-particle diffusion resistance affecting adsorption was explored by use of the intra-particle diffusion model.[47] Intra-particle diffusion was characterized using the relationship between specific sorption (q_t) and the square root of time ($t^{1/2}$). This relation is expressed as follows:[47]

$$q_t = k_{id} t^{1/2} + I \qquad (11)$$

where q_t is the quantity of ACP adsorbed at time t (mg g^{-1}) and k_{id} is the intra-particle diffusion rate constant (g mg^{-1} min$^{-1/2}$); a plot of q_t *vs.* $t^{1/2}$ should be a straight line with a slope k_{id} and intercept I when the adsorption mechanism follows an intra-particle diffusion process. The value of the intercept gives an idea about the thickness of boundary layer, *i.e.*, the larger the intercept, the greater is the boundary layer affect.[49] Plots of mass of ACP pesticide adsorbed per unit mass of adsorbent, q_t, *versus* $t^{1/2}$ are presented in Fig. 10. The deviations of the straight lines from the origin may be due to differences in rate of mass transfer in the initial and final stages of adsorption.[50] Furthermore, such deviations of the straight lines from the origin indicate that pore diffusion is not the sole rate-controlling step,[51] as was deduced earlier by the Bangham Equation. From Fig. 10, it may be seen that there are two separate regions – the first straight portion is attributed to macropore diffusion (phase I) and the second linear portion to micropore diffusion (phase II).[52] These show only the pore diffusion data. Phase I is attributed to the instantaneous utilization of the most readily available adsorption sites on the adsorbent surface. Phase II may be attributed to the very slow diffusion of the adsorbate from the surface film into the micropores, which are the least accessible adsorption sites. This also stimulates a very slow rate of migration of adsorbate from the liquid phase on to the surface of the adsorbents. That the values of $k_{id,2}$ are lower than those of $k_{id,1}$ implies that ACP diffuses into the pores of the adsorbents. As the diffusion resistance increases with time, the diffusion rate decreases. Thus, the adsorption is a multi-step process involving transport of ACP to the surface of the adsorbents followed by its diffusion into the interior of the pores.

CONCLUSIONS

MZBFA was formed by the hydrothermal alkaline treatment of BFA. The microwave irradiation of the reaction solution was effective in enhancing the zeolitization. This was assign to the stimulated dissolution of SiO_2 and Al_2O_3 from BFA by the rapid heating rate and probably by the strong attack of the glass phase by the active water molecules. On the other hand, microwave heating in the middle stage significantly retarded the formation of zeolite. This was caused by impeded nucleation in the intermediate aluminosilicate gel. Therefore, early-stage microwave heating followed by conventional heating was effective in enhancing the zeolization from Bagasse fly ash. The microwave heating was a very effective method of modifying the porosity and the surface chemistry of BFA. In addition, after microwave treatment, the surface of MZBFA remained in a more reactive state and thus exhibited a higher adsorption capacity. The adsorbents were characterized by the FTIR, PXRD and SEM techniques and possessed improved morphological and adsorption properties. The PXRD analysis data confirmed the formation of zeolites P and X as the major minerals.

Batch experiments revealed that solute removal was favored at lower solute concentrations, increased contact time, increased adsorbent dose and higher temperature at the acidic pH of 2. Equilibrium was attained in 240 min for a dose of 3 g L^{-1} and an ACP concentration of 125 mg L^{-1}. A thermodynamics study proved that the adsorption process was endothermic and spontaneous. The kinetics of the adsorption process was found to follow the pseudo-second-order kinetic model. The Langmuir isotherm fitted the batch experimental data, indicating monolayer coverage of the outer surface of the adsorbents by ACP molecules. MZBFA showed a higher adsorption capacity for ACP than the native BFA. The mass transfer and rate expression studies confirmed that the rate of adsorption was associated with mass transfer from the bulk liquid to the external surface of the particles and intra-particle diffusion from the adsorbent surfaces.

The results demonstrated that BFA, which has a very low economic value, might be effectively used for the synthesis of zeolitic materials that exhibited extractive efficacy for ACP from aqueous solutions.

И З В О Д

ЕФИКАСНОСТ ЕКСТРАКЦИЈЕ АЦЕФАТА МИКРОТАЛАСНО СИНТЕТИСАНИМ ЗЕОЛИТИМА: РАВНОТЕЖА И КИНЕТИКА

BHAVNA A. SHAH[1], AJAY V. SHAH[2] и PIYUSH Y. JADAV[1]

[1]*Department of Chemistry, Veer Narmad South Gujarat University, Surat-395007, Gujarat, India* и [2]*Science and Humanity Department, Polytechnic, Vidyabharti trust, Umrakh, Bardoli-394345, Gujarat, India*

Приказано је истраживање примене Bagasse летећег пепела (Bagasse fly ash, BFA), одпадног материјала у индустрији добијања шећера из шећерне трске, као и зеолитног материјала (MZBFA), синтетисаног из BFA комбиновањем конвенционалног и микроталасног рефлукс метода, као адсорбента за екстракцију ацефата – ACP (органофосфорног пестицида) из водених раствора. Синтетисани адсорбент је карактерисан различитим методама, као што су FTIR, PXRD и SEM. Утицај експерименталних параметара истраживан је применом шаржних адсорпционих техника за екстракцију ACP. Показано је да се степен екстракције повећава са смањењем почетне концентрације ACP, као и са смањењем величине честица адсорбента. Процес је брз и равнотежа се успоставља у времану од 90 min. Експериментални подаци су фитовани моделима псеудо-првог и псеудо-другог реда, *Bangham*-овим моделом, као и моделом интра-честичне дифузије. Моделом псеудо-другог реда је могућ реалан опис кинетике процеса адсорпције. Од више промењених модела, равнотежне податке најбоље описује Ленгмирова (*Langmuir*) изотерма. Термодинамичка анализа показује да је адсорпија ACP већа на MZBFA него на BFA. Може се закључити да је синтетисани зеолит јефтина и погодна алтернатива *Bagasse* летећем пепелу као адорбенту за уклањање пестицида из отпадних вода.

(Примљено 30. маја, ревидирано 23. новембра 2012)

REFERENCES

1. N. P. Agnihotri, *Pesticide: Safety Evaluation and Monitoring*, All India Coordinated Project (AICRP) on Pesticide Residues; Indian Agricultural Research Institute, New Delhi, India, 1999, p. 132

2. M. T. Meyer, E. Thurman, in *Herbicide Metabolites in Surface Water and Groundwater*, M. T. Meyer, E. Thurman, Eds., *ACS Symp. Ser.* **630** (1996) 1
3. A. Adeyeye, O. Osibanjo, *Sci. Total Environ.* **231** (1999) 227
4. C. Hura, M. Leanca, L. Rusu, B. A. Hura, *Toxical Lett.* **107** (1999) 103
5. K. James, W. D. Guenzi, *Pesticides in Soil and Water*, Soil Science Society of America, Madison, WI, 1986
6. C. Bolognesi, G. Morasso, *Trends Food Sci. Technol.* **11** (2000) 182
7. I. Ali, C. K. Jain, *Curr. Sci.* **75** (1998) 123
8. F. J. Beltrán, J. F. Garcia-Araya, B. Acedo, *Water Res.* **28** (1994) 2153
9. *Milieukwaliteitsnormen bodem, water, lucht*, in *(Inter)national normen stoffen*, Ministerie van Volkshuisvesting, Ruimtelijke Ordening en Milieu (Ministry of Housing, Spatial Planning and the Environment), VROM, 1997 (in Dutch)
10. A. Topalov, B. Abramovic, D. Monlar-Gabor, J. Csanadi, O. Arcson, *J. Photochem. Photobiol., A* **140** (2001) 249
11. C. Zwiener, L. Weil, R. Niessner, *Int. J. Anal. Chem.* **58** (1995) 247
12. J. B. Weber, H. D. Coble, *J. Agric. Food Chem.* **16** (1968) 475
13. M. A. El-bid, O. A. Aly, *Water Res.* **11** (1977) 611
14. V. K. Gupta, I. Ali, in Adsorbents for water treatment: Low cost alternatives to carbon, in Encyclopedia of Surface and Colloid Science, A. Hubbard, Ed., Marcel Dekker, New York, 2002, p. 136
15. H. Jian-Ying, A. Takako, O. Yutaka, M. Takeshi, M. Yasumoto, *Water Res.* **32** (1998) 2593
16. V. K. Gupta, I. Ali, *Water Res.* **35** (2001) 33
17. V. K. Gupta, I. Ali, S. Suhas, V. K. Saini, *J. Colloid Interface Sci.* **299** (2006) 556
18. V. F. Domingues, G. Priolo, A. C. Alves, M. F. Cabral, C. Delerue-Matos, *J. Environ. Sci. Health, B* **42** (2007) 649
19. J. Boucher, L. Steiner, I. W. Marison, *Water Res.* **41** (2007) 3209
20. M. Akhtar, S. M. Hasany, M. I. Bhanger, S. Iqbal, *Chemosphere* **66** (2007) 1829
21. I. Ali, V. K. Gupta, *Nat. Protoc.* **1** (2006) 2661
22. V. C. Srivastava, *M. Tech. Dissertation*, Indian Institute of Technology Roorkee, India, 2003
23. I. D. Mall, S. Tewari, N. Singh, I. M. Mishra, in Proceeding of the eighteenth international conference on solid waste technology and management, Philadelphia, PA, USA, 2003, p. 23
24. V. K. Gupta, C. K. Jain, I. Ali, M. Sharma, V. K. Saini, *Water Res.* **37** (2003) 4038
25. V. K. Gupta, I. Ali, *Sep. Purif. Technol.* **18** (2000) 131
26. B. A. Shah, A. V. Shah, H. D. Patel, *Environ. Prog. Sustain. Energy* **30** (2011) 549
27. H. Freundlich, *Z. Phys. Chem.* **57** (1906) 384
28. I. Langmuir, *J. Am. Chem. Soc.* **40** (1918) 1361
29. M. M. Dubinin, E. D. Zaverina, L. V. Radushkevich, *Zh. Fiz. Khim.* **21** (1947) 1351
30. M. J. Temkin, V. Pyzhev, Acta Physicochim. URSS **12** (1940) 217
31. S. Brunauer, P. H. Emmett, E. Teller, *J. Am. Chem. Soc.* **60** (1938) 309
32. E. P. Barrett, L. G. Joyner, P. P. Halenda, *J. Am. Chem. Soc.* **73** (1951) 373
33. J. S. Noh, J. A. Schwarz, *Carbon* **28** (1990) 675
34. D. Vucinic, I. Miljanovic, A. Rosic, P. Lazic, *J. Serb. Chem. Soc.* **68** (2003) 471
35. Y. Wang, Y. Guo, Z. Yang, H. Cai, Q. Xavier, *Sci. China, D* **46** (2003) 967
36. *Joint committee on powder diffraction standards*, Index Inorganic to the powder diffraction file, Publication PDIS-211, Newton Square, PA, 1971

37. M. Inada, H. Tsujimoto, Y. Eguchi, N. Enomoto, J. Hojo, *Fuel* **84** (2005) 1482
38. B. Pan, W. Du, W. Zhang, X. Zhang, Q. Zhang, B. Pan, L. Lv, Q. Zhange, J. Chen, *Environ. Sci. Technol.* **41** (2007) 5057
39. A. Bhatnagar, *J. Hazard. Mater.* **139** (2007) 93
40. E. Tutem, R. Apak, C. F. Unal, *Water Res.* **32** (1998) 2315
41. I. D. Mall, V. C. Srivastava, M. M. Swamy, B. Prasad, I. M. Mishra, *Colloids Surf., A* **272** (2006) 89
42. *Pesticide Properties Database*, http://sitem.herts.ac.uk/aeru/footprint/en (September 2011)
43. Y. S. Ho, G. F. Malash, M. I. El-Khaiary, *Desalination* **257** (2010) 93
44. S. Lagergren, *Kungl. Svenska Vetenskapsakad. Handl.* **24** (1898) 1
45. Y. S. Ho, G. McKay, *Process Biochem.* **34** (1999) 451
46. E. Tutem, R. Ape, C. F. Unal, *Water Res.* **32** (1998) 2315
47. W. J. Weber Jr., J. C. Morris, J. Sanit. *Eng. Div. Proceed. Am. Soc. Civil Eng.* **89** (1963) 31
48. B. A. Shah, A. V. Shah, R. R. Singh, N. B. Patel, *J. Environ. Sci. Health, A* **44** (2009) 880
49. K. Kannan, M. M. Sundaram, *Dyes Pigm.* **51** (2001) 25
50. K. K. Panday, G. Prasad, V. N. Singh, *Environ. Technol. Lett.* **50** (1986) 547
51. V. J. Poots, G. McKay, J. J. Healy, *J. Water Pollut. Control Fed.* **50** (1978) 926
52. S. J. Allen, G. McKay, Y. H. Khader, *Environ Pollut.* **56** (1989) 39.